aerospace

MDPI

Article

3D Printer Selection for Aircraft Component Manufacturing Using a Nonlinear FGM and Dependency-Considered Fuzzy VIKOR Approach

Yu-Cheng Wang [1], Tin-Chih Toly Chen [2,*] and Yu-Cheng Lin [3]

[1] Department of Aeronautical Engineering, Chaoyang University of Technology, Taichung City 413, Taiwan; tony.cobra@msa.hinet.net
[2] Department of Industrial Engineering and Management, National Yang Ming Chiao Tung University, Hsinchu City 300, Taiwan
[3] Department of Computer-Aided Industrial Design, Overseas Chinese University, 100, Chiao Kwang Rd., Taichung City 407, Taiwan; yclin@ocu.edu.tw
* Correspondence: tcchen@nycu.edu.tw

Abstract: As a viable means to enhance the sustainability and competitiveness of aircraft manufacturing and maintenance, three-dimensional (3D) printing has been extensively used in the aircraft industry. However, due to the growing number of suitable 3D printers and the often-high prices of these 3D printers, aircraft manufacturers still face many obstacles in screening possible 3D printers. In addition, dependencies between criteria make it difficult for decision makers to properly assess their absolute priorities. Existing methods fail to address these issues. To solve this problem, this study proposes a nonlinear fuzzy geometric mean (FGM) and dependency-considered fuzzy vise kriterijumska optimizacija i kompromisno resenje (fuzzy VIKOR) approach. The first novel treatment is to design the nFGM method to ensure that the absolute priorities assigned to criteria are correct. Subsequently, in the dependency-considered fuzzy VIKOR, the dependencies between criteria are considered, and a realistic reference point is defined by measuring the distance from each 3D printer to it for proper evaluation. The nonlinear FGM and dependency-considered fuzzy VIKOR approach has been applied to assess and compare five 3D printers for manufacturing aircraft components.

Keywords: 3D printing; 3D printer; fuzzy geometric mean; fuzzy VIKOR; criterion dependency

Citation: Wang, Y.-C.; Chen, T.-C.T.; Lin, Y.-C. 3D Printer Selection for Aircraft Component Manufacturing Using a Nonlinear FGM and Dependency- Considered Fuzzy VIKOR Approach. *Aerospace* **2023**, *10*, 591. https://doi.org/10.3390/aerospace10070591

Academic Editor: Spiros Pantelakis

Received: 18 March 2023
Revised: 21 June 2023
Accepted: 26 June 2023
Published: 28 June 2023

1. Introduction

Three-dimensional (3D) printing has been widely used to manufacture aircraft components due to advances in computing, sensor, and material technologies, with the main motivation being to reduce the weight of aircraft components and avoid structural weakness due to assembly [1–3]. For this purpose, new carbon fiber composite substrates and metal powder have been used in 3D printing to manufacture small aircraft components [2]. Following this trend, Airbus, one of the largest multinational aerospace companies in Europe, designs, manufactures, and sells a wide range of commercial aircraft equipped with 3D-printed parts [1]. In addition, the aircraft industry in Indian outsources certain non-strategic components that can be manufactured through 3D printing/additive manufacturing [4]. Further, Avio Aero, a major Italian company that designs, manufactures, and maintains civil and military aerospace subsystems and systems, has established a factory with more than 60 3D printers and two gas atomizers to produce in-house metal 3D printing powder [5]. The benefits of 3D printing aircraft components include low or zero waste [6], less environmental impact [7], possibility of local manufacturing [8,9], timely production (including just-in-time delivery) [10,11], higher specifications of the final product [12,13], and flexibility (such as increased production volume) [4,14–16].

However, selecting a suitable 3D printer for manufacturing aircraft components is a challenging task [17,18]. First, large 3D printers avoid assembly to improve component

quality but are often expensive. In addition, 3D printers with higher resolution can make finer products but are less efficient. In the face of such a phenomenon, decision makers have to make trade-offs.

Some related references are summarized as follows. Multi-criteria decision-making (MCDM) references on 3D printer selection are not rich. Robertson et al. [17] applied a weighted average (WA) to evaluate and compare the overall performances of 3D printers. In addition, fuzzy, probabilistic, or gray sets were employed in order to take into account the subjective assessments of experts when evaluating 3D printers. Prabhu and Ilangkumaran [19] apply the fuzzy vise kriterijumska optimizacija i kompromisno resenje (fuzzy VIKOR) method to evaluate and rank 3D printers. Subsequently, for the same purpose, Prabhu and Ilangkumaran [20] combined gray analysis with the technique for order preference by similarity to the ideal solution (TOPSIS). Lin and Chen applied the fuzzy analytic hierarchy process (FAHP) and fuzzy TOPSIS jointly to select a suitable bioprinter. Lei et al. [21] proposed the probabilistic double hierarchy linguistic (PDHL)-evaluation based on the distance from average solution (EDAS) method to evaluate 3D printers.

Existing methods in this field suffer from the following drawbacks:

- Several MCDM methods [19,21] use complex calculations to derive the priorities of criteria, which is difficult to understand and communicate and goes against the idea of explainable artificial intelligence (XAI) [22];
- Some existing methods are illustrated with numerical examples rather than real cases;
- As mentioned above, the performances of 3D printers in different aspects may be correlated, while existing methods assume that they are independent.

To solve these problems, this study proposes a nonlinear fuzzy geometric mean (nFGM) and dependency-considered fuzzy VIKOR approach for assisting aircraft manufacturers in choosing suitable 3D printers. In the proposed methodology, first, the nonlinear fuzzy geometric mean (nFGM) method is devised to ensure that the absolute priorities of criteria are properly derived. The fuzzy priorities of criteria are fed into fuzzy VIKOR [19,23] to assess and compare the overall performances of 3D printers, in which the dependency between criteria is considered when defining the reference point to measure the distance between a 3D printer and it. Table 1 highlights the distinction between the proposed methodology and some selected references, where the accuracy of a method is evaluated by the mean absolute deviation (MAD) in deriving the fuzzy priorities of criteria, while the efficiency is measured in terms of the execution time.

Table 1. Distinction between the proposed methodology and several selected references.

Method	Method for Deriving Criteria	Method for Evaluating Alternatives	Accuracy	Efficiency	Dependency between Criteria
Lin and Chen [14]	Fuzzy geometric mean (FGM)-Fuzzy intersection (FI)	FTOPSIS	Low	High	Not considered
Robertson et al. [17]	Subjective assignment	WA	Low	Very high	Not considered
Prabhu and Ilangkumaran [19]	FGM	Fuzzy VIKOR	Low	High	Not considered
Prabhu and Ilangkumaran [20]	Grey analysis	TOPSIS	Not comparable	Medium	Not considered
Lei et al. [21]	PDHL	EDAS	Low	High	Not considered

Table 1. *Cont.*

Method	Method for Deriving Criteria	Method for Evaluating Alternatives	Accuracy	Efficiency	Dependency between Criteria
Chen [24]	Efficient approximating alpha-cut operations (xACO)	Type-II fuzzy VIKOR	High	Low	Not considered
The proposed methodology	nFGM	Dependency-considered fuzzy VIKOR	High	High	Considered

The contribution of this study resides in

- The nFGM method is devised to derive the absolute priorities of criteria. In this way, the derivation accuracy can be enhanced without reducing efficiency;
- By considering the dependency between criteria, the defined reference points are reasonable and realizable, thereby improving the correctness of decision making.

The following sections are devoted to various purposes. Section 2 is a review of 3D printing technologies with applications in manufacturing and repairing aircraft parts. Section 3 introduces the nFGM and dependency-considered fuzzy VIKOR approach proposed in this study. Section 4 presents the details of applying the nFGM and dependency-considered fuzzy VIKOR approach to assess five 3D printers that have been widely used in the automotive and aircraft industries for manufacturing aircraft components based on five attributes (the number of materials supported, the number of nozzles, price, resolution, and speed). The application results of four existing methods utilizing different derivation and assessment techniques were also reported. Section 5 draws some conclusions from the experimental results and lists some topics to exploit more complex dependencies between criteria or to ensure repeatability and traceability of the 3D printing process for fair comparison in the future.

2. 3D Printing Technologies for Manufacturing Aircraft Components

Direct metal laser sintering (DMLS), also known as direct laser metal forming (DLMF), is a 3D printing technique that follows a computer-aided design (CAD) file to direct a high-intensity laser beam onto a bed of metal powder to fuse metal particles [25]. DMLS has been widely applied to manufacturing aircraft components. For example, martensitic 17-4 precipitation-hardenable stainless steel has been developed for the manufacture of aircraft structural components such as slat rails, flap rails, etc. However, maintaining a uniform thickness in aircraft structural components is difficult using conventional machining. Singh et al. [26] applied DMLS to solve this problem and optimized the setup of 3D printers through a series of experiments. Śliwa et al. [27] fabricated several aircraft parts from titanium alloy using the DMLS technology, followed by the scanning electron microscope (SEM) analysis of the microstructure of surface fragments of polished and etched samples and Vickers hardness tests.

SLM (Selective Laser Melting) and DMLS are two very similar powder bed fusion (PBF) technologies. Both technologies use a laser beam to melt metal powder in a specified pattern. By repeating this process in successive layers, 3D printers build complex parts, often using advanced metal alloys. For example, Ferro et al. [28] applied SLM to fabricate lightweight panels for aircraft wings. By integrating all functional components into a single piece, the overall weight and operating costs were reduced while the strength was increased.

Laser cladding, also known as laser metal deposition, is a 3D printing technology that adds one material to the surface of another [29]. Laser cladding is the process of feeding a stream of metal powder or wire into the molten pool created when a laser beam scans

the target surface to deposit a coating of the material of choice. Laser cladding is another 3D printing technology that has been widely applied to the aircraft industry, especially in the repair and maintenance of aircraft parts. For example, Liu et al. [30] developed a laser cladding-based metal deposition technique to reduce corrosion and restore the structural geometry of aluminum alloy aircraft structures. Song et al. [31] investigated the effectiveness of applying laser cladding to improve the crack resistance and damage tolerance of aluminum alloy aircraft structures. According to their experimental results, higher laser power or lower laser scanning speed could improve the fatigue life of laser-treated samples.

Binder jetting is a powder-based 3D printing technique in which a liquid polymer binder is selectively deposited onto a powder bed, joining metal particles and forming a green body [32]. Binder jetting also has many applications in the manufacture of aircraft parts. For example, Gupta et al. [33] examined the feasibility of fabricating the main landing gear from Al6061 T6 using binder jetting 3D printing technology. Tang et al. [34] compared the energy consumption and CO_2 emissions of a binder-jet aircraft engine bracket with that manufactured using a conventional computer numerical control (CNC) milling process. Experimental results showed that 3D-printed aircraft engine brackets reduced energy consumption by 23% and CO_2 emissions by 53%.

Electron beam melting (EBM) places metal powders or wires under a vacuum and fuses them together by heating them using an electron beam [35]. EBM differs from SLS because the raw material is completely melted. EBM has been widely applied in the production of airframe parts [36]. According to Petrovic and Niñerola [37], the recyclability of atomized Ti-6Al-4V powder used as raw material in EBM meets aerospace standards. Prikhna et al. [38] investigated the feasibility of using EBM to fabricate thermal barrier coatings for aircraft engine blades from oxidation-resistant CoCrAlY alloys. The structure, chemistry, and phase composition of oxidation-resistant CoCrAlY alloys were investigated.

Fused deposition modeling (FDM) is a 3D printing technology in which materials are extruded through a nozzle and joined together to create 3D objects. FDM is probably the most popular 3D printing technology and has been widely used to build aircraft component models. For example, Budzik [39] examined the geometric accuracy of an aircraft engine blade model built using two 3D printing techniques: FDM and stereolithography (SLA). Experimental results showed that SLA achieved higher geometric accuracy than FDM.

Multi-jet fusion (MJF) is a powder bed fusion (PBF) technology that uses a heat source to fuse particles together in a build chamber filled with thermoplastic powder. Printed 3D objects have a good surface finish, fine feature resolution, and consistent mechanical properties. MJF is one of the newer 3D printing technologies on the market and holds great potential for manufacturing aircraft components. For example, Nazir et al. [40] examined the energy absorption, stiffness, and deflection of helical springs of various dimensions fabricated using MJF. The experimental results showed that the shape of the helical spring had a significant effect on its performance.

Compared to EBM, BJ may take more time to print a single unit due to additional steps such as curing and sintering [41]. In addition, DMLS has many advantages over EBM, such as higher resolution, more materials available for printing, lower beam power required, etc. [42]. For these reasons, most of the 3D printers compared in this study used DMLS, and no 3D printers using BJ or EBM were compared.

3. Methodology

The nFGM and dependency-considered fuzzy VIKOR approach includes the following steps:

Step 1. Form the fuzzy pairwise comparison matrix and check its fuzzy consistency ratio;
Step 2. Apply nFGM to derive the absolute priorities of criteria;
Step 3. Apply the formulae of the criteria to assess the performances of each 3D printer;
Step 4. Assess and compare 3D printers using dependency-considered fuzzy VIKOR;
Step 5. Choose the 3D printer that surpasses the other alternatives.

Figure 1 describes the procedure by which the nFGM and the dependency-considered fuzzy VIKOR approach are implemented.

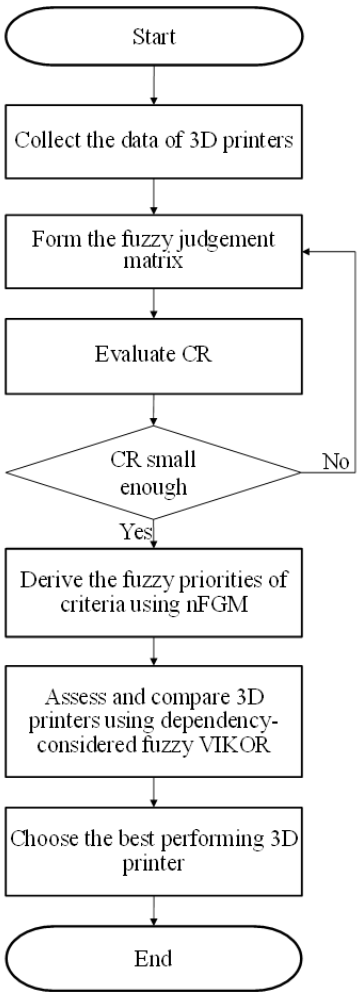

Figure 1. Implementation process of the nFGM and dependency-considered fuzzy VIKOR approach.

3.1. nFGM for Deriving the Fuzzy Priorities of Criteria

At first, the decision maker forms the fuzzy pairwise comparison matrix $\widetilde{\mathbf{A}} = \{\widetilde{a}_{ij}\}$; The following equations can be solved to derive the absolute priorities of criteria [23,43]:

$$det\left(\widetilde{\mathbf{A}}(-)\widetilde{\lambda}\mathbf{I}\right) = 0 \tag{1}$$

$$\left(\widetilde{\mathbf{A}}(-)\widetilde{\lambda}\mathbf{I}\right)(\times)\widetilde{\mathbf{x}} = 0 \tag{2}$$

where $\widetilde{\lambda}$ is the fuzzy eigenvalue, and $\widetilde{\mathbf{x}}$ is the associated eigenvector. $(-)$ and $(\times)$ are operations of subtracting and multiplying triangular fuzzy numbers (TFNs), respectively. The function det() is to calculate the determinant of a matrix. Then, the fuzzy priorities of criteria i, $\widetilde{w}_i$, is equal to

$$\widetilde{w}_i = \frac{\widetilde{x}_i}{\sum_{l=1}^{n} \widetilde{x}_l} \tag{3}$$

However, the fuzzy multiplication operations make Equations (1) and (2) intractable. To solve this problem, most past studies applied approximation methods such as fuzzy geometric mean (FGM) [18], fuzzy extent analysis (FEA) [1], or fuzzy inverse of column sum method (FICSM) to approximate the values of absolute priorities. However, imprecise fuzzy

priorities may eventually lead to wrong decisions. Conversely, it is theoretically possible that the exact values of absolute priorities can be derived using alpha-cut operations (ACO) [18]. For a fuzzy pairwise comparison matrix of size $n \times n$, $\nu 2^{C_2^n}$ crisp eigen analyses are required, where ν is the number of α levels considered. However, ACO is inefficient if there are more than seven criteria. To address this issue, Chen et al. [44] proposed the approximating ACO method (xACO) that attempts to fit the half-membership functions of an absolute priority without enumerating all possible combinations of α cuts. However, even considering only 10% of the α-cut combinations, xACO still takes a lot of time.

Recently, some efforts have been made to improve the approximation accuracy using FGM. For example, Chen et al. [43] proposed cFGM, where fuzzy priorities approximated by FGM are calibrated using a crisp eigen analysis that only considers the cores of $\widetilde{a}_{ij}$ (i.e., a_{ij2}). Chen et al. [43] proposed the calibrated piecewise-linear FGM (cpFGM) approach, in which the membership function of an absolute priority is approximated by a piecewise-linear function by connecting the α cuts of $\widetilde{w}_i$ for several α levels. Wu et al. [23] proposed acFGM, in which both sides of the membership function can be adjusted using different functions (i.e., additive or multiplicative functions). The nFGM method proposed in this study aims to approximate the membership function of an absolute priority with a nonlinear function. A comparison of various methods is summarized in Table 2. As mentioned previously, the accuracy of a method can be evaluated by the MAD in deriving the fuzzy priorities of criteria, and the efficiency is measured in terms of the execution time [44].

Table 2. Comparison between FGM variants and ACO variants.

Method	Number of Crisp Eigen Analyses Required	Number of FGM Calculations Required	Shape of Membership Function	Efficiency	Accuracy
ACO	$\nu 2^{C_2^n}$	0	Nonlinear	Very low	Very high
xACO	10% $\nu 2^{C_2^n}$	0	Nonlinear	Very low~Low	High~Very high
FGM	0	1	Linear	Very high	Very low~Very high *
cFGM	1	1	Linear	High	Low~Very high *
cpFGM	1	$2\lambda - 1$	Piecewise linear	High	Moderate~Very high *
acFGM	1	1	Linear	High	Moderate~Very high *
nFGM	1	1	Nonlinear	High	High~Very high *

*: if the fuzzy pairwise comparison matrix is fully consistent.

xACO also fits the membership function of an absolute priority with a nonlinear function. The differences between xACO and nFGM reside in

- xACO is based on the actual α cuts of a fuzzy priority, while nFGM is based on the estimated α cuts to save time;
- In xACO, the half-membership function of an absolute priority is approximated by a logarithmic function, while in nFGM, the half-membership function is approximated by either an exponential or a logarithmic function.

nFGM is composed of five steps:

Step 1. Approximate the α cuts of $\widetilde{w}_i$ for α = 0, 0.5, and 1;
Step 2. Conduct a crisp eigen analysis using the cores of matrix elements: The result is indicated with $w_i(\text{crisp})$;
Step 3. Calibrate $\widetilde{w}_i$ as [43]:

$$\widetilde{w}_i \leftarrow \widetilde{w}_i \cdot \frac{w_i(\text{crisp})}{w_i^{L/R}(1)} \tag{4}$$

where $w_i^{L(R)}(\alpha)$ is the left (right) α cut of $\widetilde{w}_i$. $\widetilde{w}_i$ is updated to the right-hand side of Equation (3);

Step 4. Use the α cuts of $\widetilde{w}_i$ for α = 0 and 1 to fit both types of functions as:

$$\hat{\mu}_{\widetilde{w}_i}(x) = \begin{cases} \xi_1 e^x + \zeta_1 & if \quad w_i^L(0) \le x < w_i^{L/R}(1) \\ \xi_2 e^x + \zeta_2 & if \quad w_i^{L/R}(1) \le x < w_i^R(0) \\ 0 & otherwise \end{cases} \tag{5}$$

or

$$\hat{\mu}_{\widetilde{w}_i}(x) = \begin{cases} \xi_3 \ln(x) + \zeta_3 & if \quad w_i^L(0) \le x < w_i^{L/R}(1) \\ \xi_4 \ln(x) + \zeta_4 & if \quad w_i^{L/R}(1) \le x < w_i^R(0) \\ 0 & otherwise \end{cases} \tag{6}$$

$\hat{\mu}_{\widetilde{w}_i}(x)$ is the approximated membership function of $\widetilde{w}_i$. $\xi_1 \sim \xi_4$, $\zeta_1 \sim \zeta_4$ are real constants. In Equation (5), both sides are exponential functions. Both sides of Equation (6) are logarithmic functions. Conversely, the α cuts of $\widetilde{w}_i$ can be derived as follows:

$$w_i(\alpha) = [\ln(\frac{\alpha - \zeta_1}{\xi_1}),\ \ln(\frac{\alpha - \zeta_2}{\xi_2})] \tag{7}$$

or

$$w_i(\alpha) = [e^{\frac{\alpha - \zeta_3}{\xi_3}},\ e^{\frac{\alpha - \zeta_4}{\xi_4}}] \tag{8}$$

both are intervals. The following theorem can be applied to derive the parameters in both models.

Theorem 1.

$$\xi_1 = \frac{1}{e^{w_i^{L/R}(1)} - e^{w_i^L(0)}} \tag{9}$$

$$\zeta_1 = -\frac{e^{w_i^L(0)}}{e^{w_i^{L/R}(1)} - e^{w_i^L(0)}} \tag{10}$$

$$\xi_2 = \frac{1}{e^{w_i^{L/R}(1)} - e^{w_i^R(0)}} \tag{11}$$

$$\zeta_2 = -\frac{e^{w_i^R(0)}}{e^{w_i^{L/R}(1)} - e^{w_i^R(0)}} \tag{12}$$

$$\xi_3 = \frac{1}{\ln w_i^{L/R}(1) - \ln w_i^L(0)} \tag{13}$$

$$\zeta_3 = -\frac{\ln w_i^L(0)}{\ln w_i^{L/R}(1) - \ln w_i^L(0)} \tag{14}$$

$$\xi_4 = \frac{1}{\ln w_i^{L/R}(1) - \ln w_i^R(0)} \tag{15}$$

$$\zeta_4 = -\frac{\ln w_i^R(0)}{\ln w_i^{L/R}(1) - \ln w_i^R(0)} \tag{16}$$

Proof. The required proof is trivial. □

Step 5. Determine the function type using the α cuts of $\widetilde{w}_i$ when α = 0.5:

$$\hat{\mu}_{\widetilde{w}_i}(x) = \begin{cases} \xi_1 \ln(x) + \zeta_1 & if \quad \left|\xi_1 \ln w_i^L(0.5) + \zeta_1 - 0.5\right| \le \left|\xi_3 e^{w_i^L(0.5)} + \zeta_3 - 0.5\right| \\ \xi_3 e^x + \zeta_3 & otherwise \end{cases} \tag{17}$$

when $w_i^L(0) \le x < w_i^{L/R}(1)$, or

$$\hat{\mu}_{\widetilde{w}_i}(x) = \begin{cases} \xi_2 \ln(x) + \zeta_2 & if \quad \left|\xi_2 \ln w_i^L(0.5) + \zeta_2 - 0.5\right| \le \left|\xi_4 e^{w_i^L(0.5)} + \zeta_4 - 0.5\right| \\ \xi_4 e^x + \zeta_4 & otherwise \end{cases} \tag{18}$$

when $w_i^{L/R}(1) \le x < w_i^R(0)$.

3.2. Dependency-Considered Fuzzy VIKOR for Assessing 3D Printers

There are at least three ways to consider the dependency between criteria in MCDM in the literature: the analytic network process (ANP) way [45], the principal component analysis (PCA) way [46], and the quality function deployment (QFD) way [47].

ANP is the extension of the analytic hierarchy process (AHP). In ANP, a supermatrix of pairwise comparisons is constructed. A criterion may have different priorities for different alternatives. Therefore, the dependency between criteria is subjective and may not be easily quantified:

$$\widetilde{\omega}_i = f_{ANP}(\{\widetilde{w}_i\}),\ i = 1 \sim n \tag{19}$$

$f_{ANP}()$ is a linear function.

In addition, it becomes meaningless to derive a single set of priorities since the criteria are dependent. FGM can be applied to process a fuzzy pairwise comparison supermatrix [48]. In this way, fuzzy priorities can be derived, and alternatives can be assessed simultaneously.

PCA forms new criteria with the weighted sum of the original criteria:

$$\widetilde{\omega}_p = \textstyle\sum_{j=1}^{n} \beta_j \widetilde{w}_j,\ p = 1 \ \sim \ P \tag{20}$$

$$r_{\widetilde{\omega}_p, \widetilde{\omega}_r} = 0,\ p \ \neq \ r;\ p,\ r = 1 \ \sim \ P \tag{21}$$

$\widetilde{\omega}_p$ is the priority of new criterion p; $p = 1 \sim P$. Any two new criteria are independent, so their correlation coefficient is zero, as depicted in Equation (21).

In QFD, new and independent criteria are defined by combining the original criteria using pre-specified rules. These rules, either linear or nonlinear, are quantifiable. The dependencies between the original criteria are also taken into account. Then, pairwise comparisons are performed on the new criteria:

$$\widetilde{\omega}_p = f_{QFd}(\{\widetilde{w}_i\}),\ p = 1 \ \sim \ P \tag{22}$$

$f_{QFD}()$ is a real function.

However, the first way is purely subjective, while in other ways, the overall performance of a 3D printer does not directly map to the original criteria, which is not in line with the trend of XAI. To solve this problem, this study proposes the fourth way, which is to define multiple reference points instead of changing the original criteria:

Fuzzy VIKOR is an MCDM method that is often used to assess the overall performances of alternatives considering subjective, uncertain, or qualitative judgments [19,24,49]. In fuzzy VIKOR, a reference point (the ideal solution $\widetilde{\mathbf{\Lambda}}$) is used, usually determined as

$$\widetilde{\Lambda}_i = \max_q \widetilde{p}_{qi} \tag{23}$$

where $\widetilde{p}_{qi}$ is the performance of alternative q in optimizing criterion i. However, if there is a dependency between two criteria, it is impractical to define them in this way. For example, the cost of a 3D printer increases as the quality of the product improves. To solve this problem, two ideal solutions are defined. Furthermore, the ideal performances of two dependent criteria are defined at the same time.

If two criteria, i and j, change in opposite directions, the ideal performances of the two criteria are either

$$(\widetilde{\Lambda}_{i(1)},\ \widetilde{\Lambda}_{j(1)}) = (\max_{q} \widetilde{p}_{qi},\ \max_{q,\widetilde{p}_{qi}=\max_{k} \widetilde{p}_{qk}} \widetilde{p}_{qj}) \tag{24}$$

or

$$(\widetilde{\Lambda}_{i(2)},\ \widetilde{\Lambda}_{j(2)}) = (\max_{q,\widetilde{p}_{qj}=\max_{k} \widetilde{p}_{qk}} \widetilde{p}_{qi},\ \max_{q} \widetilde{p}_{qj}) \tag{25}$$

while the ideal performances of the other criteria remain unchanged. The ideal solution closer to an alternative is referenced. Similarly, if there is a dependency among three criteria, three ideal solutions can be defined.

The overall performance of alternative q, $\widetilde{o}_q$, can be evaluated in terms of

$$\widetilde{o}_q = \eta \cdot \frac{\widetilde{S}_q(-)\min_r \widetilde{S}_r}{\max(\max_r \widetilde{S}_r) - \min(\min_r \widetilde{S}_r)}(+)(1-\eta) \cdot \frac{\widetilde{R}_q(-)\min_r \widetilde{R}_r}{\max(\max_r \widetilde{R}_r) - \min(\min_r \widetilde{R}_r)} \tag{26}$$

where $\eta \in [0,\ 1]$ is a pre-specified constant; $\widetilde{S}_q$ and $\widetilde{R}_q$ represent the average and worst performances of alternative q, respectively:

$$\widetilde{S}_q = \sum_{i=1}^{n} (\widetilde{w}_i(\times)\widetilde{d}_{qi}) \tag{27}$$

$$\widetilde{R}_q = \max_i(\widetilde{w}_i(\times)\widetilde{d}_{qi}) \tag{28}$$

where $\widetilde{d}_{qi}$ is the distance between alternative q and its reference point in terms of criterion i:

$$\widetilde{d}_{qi} = \frac{\widetilde{\Lambda}_i(-)\widetilde{p}_{qi}}{\max(\widetilde{\Lambda}_i) - \min(\min_r \widetilde{p}_{ri})} \tag{29}$$

The representative values of $\widetilde{o}_q$, $\widetilde{S}_q$, and $\widetilde{R}_q$ can be generated using the extended center-of-gravity (COG) mechanism [50]. For example,

$$COG(\widetilde{o}_q) = \frac{\int_0^1 \alpha \cdot \frac{o_q^L(\alpha)+o_q^R(\alpha)}{2} d\alpha}{\int_0^1 \alpha d\alpha} \tag{30}$$

Alternative q is the best-performing alternative if it meets the following requirements and can be recommended to the decision maker:

- $COG(\widetilde{o}_r) - COG(\widetilde{o}_q) \geq \frac{1}{Q-1}\ \forall\ r \neq q$;
- $COG(\widetilde{R}_q) = \min_r COG(\widetilde{R}_r)$ or $COG(\widetilde{S}_q) = \min_r COG(\widetilde{S}_r)$.

4. Case Study

4.1. Background

The aeronautical engineering department of a university in Taichung wanted to purchase a 3D printer for manufacturing aircraft components to support course training and laboratory research. Moreover, 3D printers for making plastic parts are faster and cheaper than 3D printers for making metal parts. However, since the applications were not limited to specific aircraft components and only required the purchase of a 3D printer, 3D printers using various printing technologies and materials were considered. However, the ensuing analysis was divided into two parts: the first compared all 3D printers, and the second compared 3D printers used to make plastic and metal parts separately.

Five 3D printers used to manufacture aircraft components were evaluated and compared using the proposed methodology. These 3D printers have been widely used in the

automotive and aircraft industries and were recommended by their suppliers (importers). Factors such as price, speed, etc., are critical as the 3D printer has not been targeted to a specific application. Once the application is identified, factors such as performance will be critical. Finally, the decision maker considered the following factors:

- Five attributes–the number of materials supported, the number of nozzles, the price, the resolution, and the speed, were comparable. However, other properties, such as the mechanical properties of 3D-printed aircraft parts (including consistency, yield stress, ultimate strength, fatigue, etc.) may be more important in practice, but it is difficult to compare the performances in these properties of 3D-printed aircraft parts manufactured by various 3D printers in practice. One possible way to solve this problem is to ask each 3D printer supplier to print samples and provide their measurement reports. However, this would not be a comparison on an equally fair basis, even if they follow the same standard;
- Except for price and resolution, if the other attributes were larger, then all the better.

The values of some attributes were open intervals or one-sided intervals, so the upper bounds of the intervals were compared.

4.2. Application of the Proposed Methodology

In the first step, the decision maker constructed the following consistent fuzzy judgment matrix:

$$\widetilde{\mathbf{A}} = \begin{bmatrix} 1 & (3,\,5,\,7) & 1/(2,\,4,\,6) & (2,\,4,\,6) & 1/(1,\,3,\,5) \\ 1/(3,\,5,\,7) & 1 & 1/(3,\,5,\,7) & (1,\,1,\,3) & 1/(3,\,5,\,7) \\ (2,\,4,\,6) & (3,\,5,\,7) & 1 & (3,\,5,\,7) & (2,\,4,\,6) \\ 1/(2,\,4,\,6) & 1/(1,\,1,\,3) & 1/(3,\,5,\,7) & 1 & 1/(2,\,4,\,6) \\ 1,\,3,\,5 & (3,\,5,\,7) & 1/(2,\,4,\,6) & (2,\,4,\,6) & 1 \end{bmatrix}$$

The consistency ratio of $\widetilde{\mathbf{A}}$ was about 0.094.

The second step of the application was the derivation of the absolute priorities of criteria using nFGM. The values of the parameters of their membership functions were obtained and are summarized in Table 3.

Table 3. Values of parameters.

Parameter	ξ_1	ζ_1	ξ_2	ζ_2	ξ_3	ζ_3	ξ_4	ζ_4
$\widetilde{w}_1$	11.43	−12.38	−4.49	6.26	1.47	3.72	−1.34	−1.48
$\widetilde{w}_2$	43.17	−44.52	−11.39	13.01	1.84	6.41	−1.09	−2.19
$\widetilde{w}_3$	3.17	−4.16	−3.01	5.90	1.72	2.23	−3.10	−1.23
$\widetilde{w}_4$	30.99	−31.80	−13.87	15.68	1.27	4.64	−1.30	−2.72
$\widetilde{w}_5$	6.44	−7.23	−3.93	6.03	1.33	2.87	−1.81	−1.54

The derivation results are shown in Figure 2. In this way, the membership functions of fuzzy priorities were approximated by either exponential or logarithmic functions that were closer to the exact membership functions than TFNs, as detailed in Table 4.

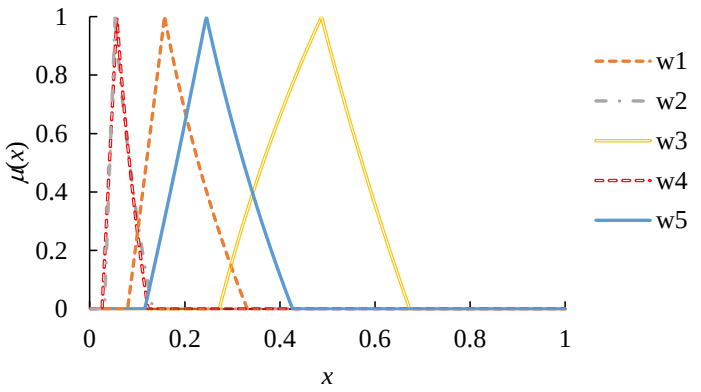

Figure 2. Fuzzy priorities of criteria derived using nFGM.

Table 4. Types of fitted memberships.

Fuzzy Priorities	Left	Right
$\widetilde{w}_1$	Exponential	Logarithmic
$\widetilde{w}_2$	Exponential	Logarithmic
$\widetilde{w}_3$	Logarithmic	Logarithmic
$\widetilde{w}_4$	Exponential	Logarithmic
$\widetilde{w}_5$	Exponential	Logarithmic

In the third step, the data of the 3D printers for manufacturing aircraft components are summarized in Table 5. The performances of these 3D printers in terms of various criteria were evaluated as real values within the interval [0, 5] [51]. The evaluation results can be referred to in Table 6.

Table 5. Data of the five 3D printers for manufacturing aircraft components.

3D Printer	Stratasys Fortus 900mc [I]	EOS M 290 [II]	Concept Laser M2 Cusing [III]	EOS M 400-4 [IV]	HP Jet Fusion 5200 [V]
Number of materials supported	7	5	4	2	5
Number of nozzles	1~4	1~2	1~2	4	2
Price (USD)	400,000~1,000,000	250,000~450,000	500,000~1,000,000	1,000,000	400,000
Printing technology	FDM	DMLS	DMLS	DMLS	MJF
Resolution (mm)	0.13 ~ 0.5	0.02 ~ 0.04	0.02 ~ 0.08	0.1 ~	0.08 ~
Speed	2230 cm^3/h	2.5 cm^3/h	2.5 cm^3/h & nozzle	100 g/h	4500 cm^3/h
Vendor	Stratasys	EOS	Concept Laser	EOS	HP

[I]: https://www.stratasys.com/3d-printers/fortus-900mc; [II]: https://www.eos.info/systems-solutions/metal/systems/eos-m-290; [III]: https://www.concept-laser.de/en/products/machine-details/m2-cusing/; [IV]: https://www.eos.info/systems_solutions/metal/systems/eos_m_400_4; [V]: https://www8.hp.com/us/en/printers/3d-printers/jet-fusion-5200-series.html (accessed on 4 January 2023).

Table 6. Evaluated performances of 3D printers.

q	$\widetilde{p}_{q1}$	$\widetilde{p}_{q2}$	$\widetilde{p}_{q3}$	$\widetilde{p}_{q4}$	$\widetilde{p}_{q5}$
1	(4, 5, 5)	(4, 5, 5)	(4, 5, 5)	(4, 5, 5)	(1.5, 2.5, 3.5)
2	(1.5, 2.5, 3.5)	(0, 0, 1)	(0, 0, 1)	(0, 0, 1)	(0, 0, 1)
3	(1.5, 2.5, 3.5)	(0, 0, 1)	(4, 5, 5)	(0, 0, 1)	(0, 0, 1)
4	(0, 0, 1)	(4, 5, 5)	(4, 5, 5)	(3, 4, 5)	(0, 0, 1)
5	(1.5, 2.5, 3.5)	(0, 0, 1)	(0, 0, 1)	(1.5, 2.5, 3.5)	(4, 5, 5)

4.2.1. Comparing All 3D Printers

In the fourth step, 3D printers were assessed and compared using dependency-considered fuzzy VIKOR. In the five attributes, price and speed were difficult to optimize

simultaneously, and therefore the dependency between the two attributes was considered in defining two reference points, as shown in Table 7.

Table 7. Two reference points.

Reference Point	$i = 1$	$i = 2$	$i = 3$	$i = 4$	$i = 5$
$\widetilde{\Lambda}_i(1)$	(4, 5, 5)	(4, 5, 5)	(4, 5, 5)	(4, 5, 5)	(1.5, 2.5, 3.5)
$\widetilde{\Lambda}_i(2)$	(4, 5, 5)	(4, 5, 5)	(0, 0, 1)	(4, 5, 5)	(4, 5, 5)

For each 3D printer, the closest reference point was found. Then, the fuzzy distance between 3D printer q and the closest reference point was measured, which is summarized in Table 8.

Table 8. Distances between each 3D printer and the closest reference point.

q	$\widetilde{d}_q$
1	(0, 0, 0.2)
2	(0.1, 0.5, 0.7)
3	(0.1, 0.5, 0.7)
4	(0.6, 1, 1)
5	(0.1, 0.5, 0.7)

Based on the two fuzzy distances, each 3D printer was assessed on the whole, for which η was set to 0.5. The evaluation results, in terms of their α cuts, are shown in Table 9. Subsequently, to facilitate the comparison of the 3D printers, the COGs of their fuzzy overall performances were also derived. The results are also shown in this table. The 3D printers were then ranked according to the defuzzified overall performances; the smaller, the better.

Table 9. Overall performance of each 3D printer.

q (3D Printer No.)	$\widetilde{o}_q$ (Overall Performance) (α: α Cut)	$D(\widetilde{o}_q)$	Rank
1	0: [0, 0.105]; 0.1: [0, 0.102]; 0.2: [0, 0.097]; 0.3: [0, 0.091]; 0.4: [0, 0.083]; 0.5: [0, 0.074]; 0.6: [0, 0.063]; 0.7: [0, 0.05]; 0.8: [0, 0.035]; 0.9: [0, 0.019]; 1: [0,0]	0.022	1
2	0: [0.19, 0.437]; 0.1: [0.22, 0.458]; 0.2: [0.252, 0.48]; 0.3: [0.288, 0.501]; 0.4: [0.328, 0.522]; 0.5: [0.37, 0.542]; 0.6: [0.417, 0.563]; 0.7: [0.467, 0.583]; 0.8: [0.521, 0.603]; 0.9: [0.58, 0.623]; 1: [0.643, 0.643]	0.531	5
3	0: [0.036, 0.171]; 0.1: [0.046, 0.181]; 0.2: [0.057, 0.19]; 0.3: [0.072, 0.198]; 0.4: [0.088, 0.204]; 0.5: [0.106, 0.21]; 0.6: [0.125, 0.214]; 0.7: [0.146, 0.217]; 0.8: [0.168, 0.218]; 0.9: [0.192, 0.218]; 1: [0.217, 0.217]	0.182	3
4	0: [0.054, 0.163]; 0.1: [0.065, 0.173]; 0.2: [0.078, 0.182]; 0.3: [0.093, 0.191]; 0.4: [0.108, 0.198]; 0.5: [0.125, 0.205]; 0.6: [0.142, 0.211]; 0.7: [0.161, 0.216]; 0.8: [0.181, 0.22]; 0.9: [0.202, 0.222]; 1: [0.224, 0.224]	0.189	4
5	0: [0.024, 0.132]; 0.1: [0.029, 0.133]; 0.2: [0.035, 0.133]; 0.3: [0.042, 0.136]; 0.4: [0.05, 0.137]; 0.5: [0.059, 0.137]; 0.6: [0.069, 0.136]; 0.7: [0.081, 0.133]; 0.8: [0.093, 0.13]; 0.9: [0.106, 0.125]; 1: [0.119, 0.119]	0.107	2

4.2.2. Comparing 3D Printers Using Different Materials

The five 3D printers were divided into two categories: 3D printers for metal parts (including EOS M 290, Concept Laser M2 Cusing, and EOS M 400-4) and 3D printers for plastic parts (including Stratasys Fortus 900mc and HP Jet Fusion 5200).

For the first category, there was only a single reference point (see Table 10). The fuzzy distance between each 3D printer for making metal parts and the reference point was measured to evaluate the overall performance of the 3D printer. The evaluation results are summarized in Table 11. The best-performing 3D printer for making metal parts was Concept Laser M2 Cusing.

Table 10. Reference point for 3D printers for making metal parts.

Reference Point	$i = 1$	$i = 2$	$i = 3$	$i = 4$	$i = 5$
$\widetilde{\Lambda}_i(1)$	(4, 5, 5)	(4, 5, 5)	(0, 0, 1)	(4, 5, 5)	(4, 5, 5)

Table 11. Overall performance of each 3D printer for making metal parts.

q (3D Printer No.)	$D(\widetilde{o}_q)$	Rank
2	0.451	3
3	0.092	1
4	0.113	2

The reference point for the second category is shown in Table 12. The fuzzy distance between each 3D printer for making plastic parts and the reference point was measured to evaluate the overall performance of the 3D printer. The evaluation results are summarized in Table 13. The best-performing 3D printer for making plastic parts was the Stratasys Fortus 900mc.

Table 12. Reference point for 3D printers for making metal parts.

Reference Point	$i = 1$	$i = 2$	$i = 3$	$i = 4$	$i = 5$
$\widetilde{\Lambda}_i(1)$	(4, 5, 5)	(4, 5, 5)	(4, 5, 5)	(4, 5, 5)	(4, 5, 5)

Table 13. Overall performance of each 3D printer for making metal parts.

q (3D Printer No.)	$D(\widetilde{o}_q)$	Rank
1	0.150	1
5	0.479	2

4.3. Discussion

From the experimental results, the following phenomena were noted and discussed:

(1) The most important criterion for the decision maker's selection of a suitable 3D printer was the price, followed by speed and the number of materials supported. In contrast, the number of nozzles was the least important criterion;
(2) The 3D printer that most conformed to the subjective judgment of the decision maker was Stratasys Fortus 900mc, which had the largest number of nozzles and comparable speed, while the price was not the highest. However, only the second requirement was met. HP Jet Fusion 5200 and Concept Laser M2 Cusing came in second and third;
(3) The superiority of the Stratasys Fortus 900mc over the other 3D printers became significant when the value of η exceeded 0.6, which meant that more emphasis was placed on the average performance rather than the worst performance.
(4) Among 3D printers that apply the direct metal laser sintering (DMLS) technology, Concept Laser M2 Cusing was the best choice;
(5) If the dependency between the two criteria was not considered, the ranks of 3D printers remained unchanged. However, the superiority of the Stratasys Fortus 900mc

became less significant. As a result, η must be set to a value greater than 0.66 to satisfy both two requirements;

(6) By considering the dependency between two attributes, 3D printers were compared with the closest reference points that were practically feasible. As a result, the distance between a 3D printer and its reference point was closer than that without considering the dependency, as shown in Figure 3.

(7) The application results of four contrasting MCDM methods are reported in Table 14: FGM–fuzzy weighted average (FWA) [52–54], the ordered weighted average (OWA) [55–57], FGM–FTOPSIS [58–63], and FGM-fuzzy VIKOR [64–67]. Clearly, the same 3D printer, Stratasys Fortus 900mc, was chosen by all methods, showing the trustability of the experimental result using the proposed methodology. However, 3D printers ranked differently in various methods. Their unequal performances in deriving the absolute priorities accounted for such difference. Defining and comparing with practically feasible solutions also accounted for such differences. For example, the EOS M 400-4 was not as good as the HP Jet Fusion 5200 for speed, and the opposite was true for resolution. Therefore, the two 3D printers were compared to different reference points, whereas in existing methods, they were compared to the same reference point. This explains why their ranking results in the proposed methodology differ from those in existing methods.

(8) Although the attributes of the 3D printers compared in this experiment were not specific to 3D printers for manufacturing aircraft components, the decision maker was from the aviation industry, so his judgment on the relative priorities of criteria was only applicable to 3D printers for manufacturing aircraft components, not general-purpose 3D printers. In addition, in previous studies such as Chen and Lin [57], the number of supported application types was critical for choosing a general-purpose 3D printer, but it was not considered in this study when choosing a suitable 3D printer for manufacturing aircraft components;

(9) The ground truth of this case study is that the EOS M 290 was dominated by other 3D printers and, therefore, could not be selected, while other 3D printers could be recommended using different MCDM methods. In addition, 3D printers performed better in more criteria, such as Stratasys Fortus 900mc and EOS M 400-4, which are more likely to be selected. The experimental results also support these facts.

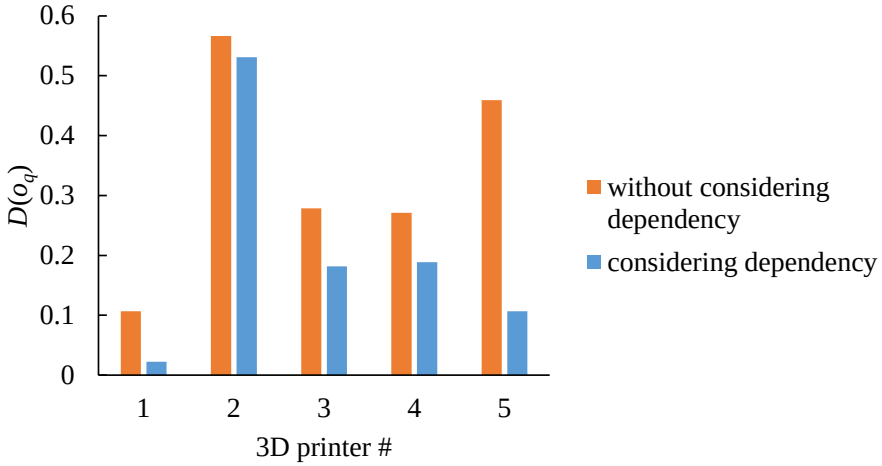

Figure 3. Distance between a 3D printer and its reference point with and without considering the dependency.

Table 14. Sequence of 3D printers in various methods.

q	Rank (FGM-FWA)	OWA	Rank (FGM-FTOPSIS)	Rank (FGM-Fuzzy VIKOR)	Rank (Proposed Methodology)
1	1	1	1	1	1
2	5	5	5	5	5
3	3	4	4	3	3
4	2	2	3	2	4
5	4	3	2	4	2

5. Conclusions

Three-dimensional printing has been extensively applied to manufacture aircraft components, bringing benefits such as low or zero waste, less environmental impact, possibility of local manufacturing, timely production, higher product quality, and flexibility. However, aircraft manufacturers still face many obstacles in screening possible 3D printers, as the options are increasingly expensive, while a decision maker may be misled by the dependency between criteria. Existing methods fail to address these issues. To solve this problem, this study proposes a nonlinear FGM and dependency-considered fuzzy VIKOR approach. In the proposed nonlinear FGM and dependency-considered fuzzy VIKOR approach; first, we devise the nFGM method so that the absolute priorities of criteria can be correctly estimated in an efficient manner. Subsequently, the fuzzy VIKOR method was modified by defining a realistic reference point considering the dependencies between criteria for evaluating the overall performance of a 3D printer.

The nonlinear FGM and dependency-considered fuzzy VIKOR approach has been applied to assess five 3D printers for manufacturing aircraft components. From the discussion results, the following points are the most important conclusions:

(1) The criterion most critical to the selection of a suitable 3D printer for manufacturing aircraft components was the price, followed by the speed and the number of materials supported;
(2) The best 3D printers using FDM, DMLS, and MJF were Stratasys Fortus 900mc, Concept Laser M2 Cusing, and HP Jet Fusion 5200V, respectively.
(3) In total, Stratasys Fortus 900mc achieved the best overall performance with an advantage of 88% over the other compared 3D printers.

The 3D printer acquired at this time lacked specific applications because the 3D printer was mainly used to support aviation education and scientific research activities. Supported courses include "Aerodynamics", "Aircraft Structural Maintenance Internship", "Engine Overhaul Internship", "Introduction to Drones", etc., that should be demonstrated with metal and plastic aircraft components or their models. If the application of the 3D printer was clearer, the considerations would be different. Printing performance and product quality will be more important criteria.

In future studies, other 3D printers for manufacturing aircraft components can be assessed in the same way. In addition, the dependencies between criteria may be much more complex than we analyzed. Furthermore, this study only compares factors that can be compared fairly and easily, and the experimental results are only used as a reference for screening suitable 3D printers. For each suitable 3D printer chosen by the proposed methodology, the supplier can be asked to print samples for further comparison. To this end, it is important to ensure the repeatability of the 3D printing process by establishing a fair qualification process [68–71]. In addition, certifiable components should be printed on demand, and all process steps should be fully traceable.

Author Contributions: Conceptualization, T.-C.T.C. and Y.-C.L.; methodology, T.-C.T.C., Y.-C.W. and Y.-C.L.; software, T.-C.T.C. and Y.-C.W.; validation, Y.-C.L.; formal analysis, T.-C.T.C. and Y.-C.W.; investigation, T.-C.T.C. and Y.-C.W.; resources, Y.-C.L.; data curation, T.-C.T.C. and Y.-C.W.; writing—original draft preparation, T.-C.T.C. and Y.-C.W.; writing—review and editing, T.-C.T.C., Y.-C.W. and Y.-C.L.; visualization, Y.-C.L.; supervision, T.-C.T.C.; project administration, T.-C.T.C. All authors have read and agreed to the published version of the manuscript.

Funding: This research received no external funding.

Data Availability Statement: Not available.

Conflicts of Interest: The authors declare that there are no conflict of interest regarding the publication of this article.

References

1. Wang, Y.-C.; Chen, T.; Yeh, Y.-L. Advanced 3D printing technologies for the aircraft industry: A fuzzy systematic approach for assessing the critical factors. *Int. J. Adv. Manuf. Technol.* **2019**, *105*, 4059–4069. [CrossRef]
2. Chung, K.-C.; Shu, M.-H.; Wang, Y.-C.; Huang, J.-C.; Lau, E.M. 3D printing technologies applied to the manufacturing of aircraft components. *Mod. Phys. Lett. B* **2020**, *34*, 2040018. [CrossRef]
3. EOS, Additive Manufacturing for Aviation Locking Shaft for the Aircraft Door of an Airbus A350. Available online: https://www.eos.info/en/all-3d-printing-applications/aerospace-3d-printing/aircraft (accessed on 3 January 2023).
4. Manda, V.R.; Kampurath, V.; Msrk, C. 3D printing and its effect on outsourcing: A study of the Indian aircraft industry. *J. Aerosp. Technol. Manag.* **2018**, *10*, e0718. [CrossRef]
5. 3DSourced.com, 3D Printing in Aerospace: Everything You Need to Know. Available online: https://www.3dsourced.com/guides/3d-printing-in-aerospace-aircraft/ (accessed on 12 January 2023).
6. Chen, T.-C.T.; Wang, Y.-C. AI applications to kaizen management. In *Artificial Intelligence and Lean Manufacturing*; Springer: Berlin/Heidelberg, Germany, 2022; pp. 37–53. [CrossRef]
7. Shuaib, M.; Haleem, A.; Kumar, S.; Javaid, M. Impact of 3D Printing on the environment: A literature-based study. *Sustain. Oper. Comput.* **2021**, *2*, 57–63. [CrossRef]
8. Chen, T.-C.T. Capacity planning for a ubiquitous manufacturing system based on three-dimensional printing. In *3D Printing and Ubiquitous Manufacturing*; Springer: Berlin/Heidelberg, Germany, 2020; pp. 47–61. [CrossRef]
9. Manners-Bell, J.; Lyon, K. The implications of 3D printing for the global logistics industry. *Transp. Intell.* **2012**, *1*, 1–5.
10. Mavri, M. Redesigning a production chain based on 3D printing technology. *Knowl. Process Manag.* **2015**, *22*, 141–147. [CrossRef]
11. Chen, T.-C.T.; Wang, Y.-C. AI applications to pull production, JIT, and production leveling. In *Artificial Intelligence and Lean Manufacturing*; Springer: Berlin/Heidelberg, Germany, 2022; pp. 55–74. [CrossRef]
12. Wu, H.-C.; Chen, T.-C.T. Quality control issues in 3D-printing manufacturing: A review. *Rapid Prototyp. J.* **2018**, *24*, 607–614. [CrossRef]
13. Chen, T.-C.T. Quality control in a 3D printing-based ubiquitous manufacturing system. In *3D Printing and Ubiquitous Manufacturing*; Springer: Berlin/Heidelberg, Germany, 2020; pp. 83–95. [CrossRef]
14. Lin, C.-W.; Chen, T. 3D printing technologies for enhancing the sustainability of an aircraft manufacturing or MRO company—A multi-expert partial consensus-FAHP analysis. *Int. J. Adv. Manuf. Technol.* **2019**, *105*, 4171–4180. [CrossRef]
15. Chen, T.-C.T. Three-dimensional printing capacity planning. In *3D Printing and Ubiquitous Manufacturing*; Springer: Berlin/Heidelberg, Germany, 2020; pp. 29–45. [CrossRef]
16. Chiu, M.-C.; Chen, T.-C.T. A ubiquitous healthcare system of 3D printing facilities for making dentures: Application of type-II fuzzy logic. *Digit. Health* **2022**, *8*, 20552076221092540. [CrossRef]
17. Roberson, D.; Espalin, D.; Wicker, R. 3D printer selection: A decision-making evaluation and ranking model. *Virtual Phys. Prototyp.* **2013**, *8*, 201–212. [CrossRef]
18. Chen, T.-C.T.; Lin, Y.-C. A FAHP-FTOPSIS approach for bioprinter selection. *Health Technol.* **2020**, *10*, 1455–1467. [CrossRef]
19. Prabhu, S.R.; Ilangkumaran, M. Decision making methodology for the selection of 3D printer under fuzzy environment. *Int. J. Mater. Prod. Technol.* **2019**, *59*, 239–252. [CrossRef]
20. Prabhu, S.R.; Ilangkumaran, M. Selection of 3D printer based on FAHP integrated with GRA-TOPSIS. *Int. J. Mater. Prod. Technol.* **2019**, *58*, 155–177. [CrossRef]
21. Lei, F.; Wei, G.; Shen, W.; Guo, Y. PDHL-EDAS method for multiple attribute group decision making and its application to 3D printer selection. *Technol. Econ. Dev. Econ.* **2022**, *28*, 179–200. [CrossRef]
22. Brito, L.C.; Susto, G.A.; Brito, J.N.; Duarte, M.A. An explainable artificial intelligence approach for unsupervised fault detection and diagnosis in rotating machinery. *Mech. Syst. Signal Process.* **2022**, *163*, 108105. [CrossRef]
23. Wu, H.-C.; Lin, Y.-C.; Chen, T.-C.T. Leisure agricultural park selection for traveler groups amid the COVID-19 pandemic. *Agriculture* **2022**, *12*, 111. [CrossRef]
24. Chen, T.-C.T. Type-II fuzzy collaborative intelligence for assessing cloud manufacturing technology applications. *Robot. Comput.-Integr. Manuf.* **2022**, *78*, 102399. [CrossRef]

25. Simchi, A.; Petzoldt, F.; Pohl, H. On the development of direct metal laser sintering for rapid tooling. *J. Mater. Process. Technol.* **2003**, *141*, 319–328. [CrossRef]
26. Singh, R.; Rishab; Sidhu, J.S. On three-dimensional printing of 17-4 precipitation-hardenable stainless steel with direct metal laser sintering in aircraft structural applications. *Proc. Inst. Mech. Eng. Part L J. Mater. Des. Appl.* **2022**, *236*, 440–450. [CrossRef]
27. Śliwa, R.E.; Bernaczek, J.; Budzik, G. The application of direct metal laser sintering (DMLS) of titanium alloy powder in fabricating components of aircraft structures. *Key Eng. Mater.* **2016**, *687*, 199–205. [CrossRef]
28. Ferro, C.G.; Varetti, S.; De Pasquale, G.; Maggiore, P. Lattice structured impact absorber with embedded anti-icing system for aircraft wings fabricated with additive SLM process. *Mater. Today Commun.* **2018**, *15*, 185–189. [CrossRef]
29. Zhu, L.; Xue, P.; Lan, Q.; Meng, G.; Ren, Y.; Yang, Z.; Xu, P.; Liu, Z. Recent research and development status of laser cladding: A review. *Opt. Laser Technol.* **2021**, *138*, 106915. [CrossRef]
30. Liu, Q.; Janardhana, M.; Hinton, B.; Brandt, M.; Sharp, K. Laser cladding as a potential repair technology for damaged aircraft components. *Int. J. Struct. Integr.* **2011**, *2*, 314–331. [CrossRef]
31. Song, M.; Wu, L.; Liu, J.; Hu, Y. Effects of laser cladding on crack resistance improvement for aluminum alloy used in aircraft skin. *Opt. Laser Technol.* **2021**, *133*, 106531. [CrossRef]
32. Li, M.; Du, W.; Elwany, A.; Pei, Z.; Ma, C. Metal binder jetting additive manufacturing: A literature review. *J. Manuf. Sci. Eng.* **2020**, *142*, 090801. [CrossRef]
33. Gupta, A.; Soni, V.; Shah, D.; Lakdawala, A. Generative design of main landing gear for a remote-controlled aircraft. *Mater. Today Proc.* **2023**. [CrossRef]
34. Tang, Y.; Mak, K.; Zhao, Y.F. A framework to reduce product environmental impact through design optimization for additive manufacturing. *J. Clean. Prod.* **2016**, *137*, 1560–1572. [CrossRef]
35. Parthasarathy, J.; Starly, B.; Raman, S.; Christensen, A. Mechanical evaluation of porous titanium (Ti6Al4V) structures with electron beam melting (EBM). *J. Mech. Behav. Biomed. Mater.* **2010**, *3*, 249–259. [CrossRef]
36. Yılmaz, F. Mechanical Characterization of Additively Manufactured Ti-6Al-4V Aircraft Structural Components Produced by Electron Beam Melting. Master's Thesis, Middle East Technical University, Ankara, Turkey, 2022. Available online: https://open.metu.edu.tr/bitstream/handle/11511/99449/index.pdf (accessed on 4 January 2023).
37. Petrovic, V.; Niñerola, R. Powder recyclability in electron beam melting for aeronautical use. *Aircr. Eng. Aerosp. Technol. Int. J.* **2015**, *87*, 147–155. [CrossRef]
38. Prikhna, T.O.; Grechanyuk, I.M.; Karpets, M.V.; Grechanyuk, M.I.; Bagliuk, G.A.; Grechanyuk, V.G.; Khomenko, O.V. Electron-beam and plasma oxidation-resistant and thermal-barrier coatings deposited on turbine blades using cast and powder Ni (Co) CrAlY (Si) alloys produced by electron-beam melting II. Structure and chemical and phase composition of cast CoCrAlY alloys. *Powder Metall. Met. Ceram.* **2022**, *61*, 230–237. [CrossRef]
39. Budzik, G. Geometric accuracy of aircraft engine blade models constructed by means of the generative rapid prototyping methods FDM and SLA. *Adv. Manuf. Sci. Technol.* **2010**, *34*, 33–43.
40. Nazir, A.; Ali, M.; Hsieh, C.H.; Jeng, J.Y. Investigation of stiffness and energy absorption of variable dimension helical springs fabricated using multijet fusion technology. *Int. J. Adv. Manuf. Technol.* **2020**, *110*, 2591–2602. [CrossRef]
41. Klein, A. How Binder Jet 3D Printing for Metals Compares to Selective Laser Melting and Electron Beam Melting. Available online: https://www.exone.com/Admin/getmedia/d2e3e618-aa7c-457a-a019-fbef2b8063c2/Klein-English-Article-012020.pdf (accessed on 21 June 2023).
42. 3DEXPERIENCE Make, DMLS vs. EBM: Differences and Comparison. Available online: https://www.3ds.com/make/solutions/blog/dmls-vs-ebm-differences-and-comparison (accessed on 21 June 2023).
43. Chen, T.; Wang, Y.-C.; Wu, H.-C. Analyzing the impact of vaccine availability on alternative supplier selection amid the COVID-19 pandemic: A cFGM-FTOPSIS-FWI approach. *Healthcare* **2021**, *9*, 71. [CrossRef]
44. Chen, T.; Lin, Y.-C.; Chiu, M.-C. Approximating alpha-cut operations approach for effective and efficient fuzzy analytic hierarchy process analysis. *Appl. Soft Comput.* **2019**, *85*, 105855. [CrossRef]
45. Aragonés-Beltrán, P.; Chaparro-González, F.; Pastor-Ferrando, J.; Rodríguez-Pozo, F. An ANP-based approach for the selection of photovoltaic solar power plant investment projects. *Renew. Sustain. Energy Rev.* **2010**, *14*, 249–264. [CrossRef]
46. Johnson, R.A.; Wichern, D.W. *Applied Multivariate Statistical Analysis*; Springer: Berlin/Heidelberg, Germany, 2002.
47. Wang, Y.-J.; Liu, L.-J.; Han, T.-C. Interval-valued fuzzy multi-criteria decision-making with dependent evaluation criteria for evaluating service performance of international container ports. *J. Mar. Sci. Eng.* **2022**, *10*, 991. [CrossRef]
48. Mikhailov, L.; Singh, M.G. Fuzzy analytic network process and its application to the development of decision support systems. *IEEE Trans. Syst. Man Cybern. Part C (Appl. Rev.)* **2003**, *33*, 33–41. [CrossRef]
49. Opricovic, S. Fuzzy VIKOR with an application to water resources planning. *Expert Syst. Appl.* **2011**, *38*, 12983–12990. [CrossRef]
50. Van Broekhoven, E.; De Baets, B. Fast and accurate center of gravity defuzzification of fuzzy system outputs defined on trapezoidal fuzzy partitions. *Fuzzy Sets Syst.* **2006**, *157*, 904–918. [CrossRef]
51. Lin, Y.-C.; Chen, T.-C.T. An intelligent system for assisting personalized COVID-19 vaccination location selection: Taiwan as an example. *Digit. Health* **2022**, *8*, 20552076221109062. [CrossRef]
52. Zheng, G.; Zhu, N.; Tian, Z.; Chen, Y.; Sun, B. Application of a trapezoidal fuzzy AHP method for work safety evaluation and early warning rating of hot and humid environments. *Saf. Sci.* **2012**, *50*, 228–239. [CrossRef]

53. Wang, Y.C.; Chen, T.C.T. A partial-consensus posterior-aggregation FAHP method—Supplier selection problem as an example. *Mathematics* **2019**, *7*, 179. [CrossRef]
54. Veerraju, N.; Prasannam, V.L.; Rallabandi, L.K. Defuzzification index for ranking of fuzzy numbers on the basis of geometric mean. *Int. J. Intell. Syst. Appl.* **2020**, *12*, 13–24. [CrossRef]
55. Lin, Y.C.; Wang, Y.C.; Chen, T.C.T.; Lin, H.F. Evaluating the suitability of a smart technology application for fall detection using a fuzzy collaborative intelligence approach. *Mathematics* **2019**, *7*, 1097. [CrossRef]
56. Linares-Mustarós, S.; Ferrer-Comalat, J.C.; Corominas-Coll, D.; Merigó, J.M. The ordered weighted average in the theory of expertons. *Int. J. Intell. Syst.* **2019**, *34*, 345–365. [CrossRef]
57. Chen, T.; Lin, C.W. Smart and automation technologies for ensuring the long-term operation of a factory amid the COVID-19 pandemic: An evolving fuzzy assessment approach. *Int. J. Adv. Manuf. Technol.* **2020**, *111*, 3545–3558. [CrossRef]
58. Merigo, J.M.; Casanovas, M. The fuzzy generalized OWA operator and its application in strategic decision making. *Cybern. Syst. Int. J.* **2010**, *41*, 359–370. [CrossRef]
59. Chen, T. Obtaining the optimal cache document replacement policy for the caching system of an EC website. *Eur. J. Oper. Res.* **2007**, *181*, 828–841. [CrossRef]
60. Noori, A.; Bonakdari, H.; Hassaninia, M.; Morovati, K.; Khorshidi, I.; Noori, A.; Gharabaghi, B. A reliable GIS-based FAHP-FTOPSIS model to prioritize urban water supply management scenarios: A case study in semi-arid climate. *Sustain. Cities Soc.* **2022**, *81*, 103846. [CrossRef]
61. Chen, T.; Chiu, M.C. Smart technologies for assisting the life quality of persons in a mobile environment: A review. *J. Ambient Intell. Humaniz. Comput.* **2018**, *9*, 319–327. [CrossRef]
62. Yadav, R.; Lee, H.H. Ranking and selection of dental restorative composite materials using FAHP-FTOPSIS technique: An application of multi criteria decision making technique. *J. Mech. Behav. Biomed. Mater.* **2022**, *132*, 105298. [CrossRef]
63. Chen, T.-C.T.; Wu, H.-C.; Hsu, K.-W. A fuzzy analytic hierarchy process-enhanced fuzzy geometric mean-fuzzy technique for order preference by similarity to ideal solution approach for suitable hotel recommendation amid the COVID-19 pandemic. *Digit. Health* **2022**, *8*, 20552076221084457. [CrossRef]
64. Rostamzadeh, R.; Govindan, K.; Esmaeili, A.; Sabaghi, M. Application of fuzzy VIKOR for evaluation of green supply chain management practices. *Ecol. Indic.* **2015**, *49*, 188–203. [CrossRef]
65. Wang, Y.-C.; Chen, T.-C.T. Analyzing the impact of COVID-19 vaccination requirements on travelers' selection of hotels using a fuzzy multi-criteria decision-making approach. *Healthc. Anal.* **2022**, *2*, 100064. [CrossRef]
66. Shemshadi, A.; Shirazi, H.; Toreihi, M.; Tarokh, M.J. A fuzzy VIKOR method for supplier selection based on entropy measure for objective weighting. *Expert Syst. Appl.* **2011**, *38*, 12160–12167. [CrossRef]
67. Chen, T.-C.T.; Lin, Y.-C. Diversified capacity planning of three-dimensional printing for a manufacturer. *Robot. Comput.-Integr. Manuf.* **2021**, *67*, 102052. [CrossRef]
68. Mukherjee, T.; DebRoy, T. A digital twin for rapid qualification of 3D printed metallic components. *Appl. Mater. Today* **2019**, *14*, 59–65. [CrossRef]
69. Wu, H.C.; Chen, T.C.T.; Huang, C.H.; Shih, Y.C. Comparing built-in power banks for a smart backpack design using an auto-weighting fuzzy-weighted-intersection FAHP approach. *Mathematics* **2020**, *8*, 1759. [CrossRef]
70. Smith, D.M.; Kapoor, Y.; Klinzing, G.R.; Procopio, A.T. Pharmaceutical 3D printing: Design and qualification of a single step print and fill capsule. *Int. J. Pharm.* **2018**, *544*, 21–30. [CrossRef]
71. Wu, H.C.; Chen, T.; Huang, C.H. A piecewise linear FGM approach for efficient and accurate FAHP analysis: Smart backpack design as an example. *Mathematics* **2020**, *8*, 1319. [CrossRef]